Monthly Notices
of the
ROYAL ASTRONOMICAL SOCIETY

Mon. Not. R. Astron. Soc. **407,** 1078–1089 (2010) doi:10.1111/j.1365-2966.2010.16907.x

Clustering of radio galaxies and quasars

E. Donoso,[1⋆] Cheng Li,[1,2] G. Kauffmann,[1] P. N. Best[3] and T. M. Heckman[4]

[1]*Max-Planck-Institut für Astrophysik, Karl-Schwarzschild-Str. 1, Postfach 1317, D-85741 Garching, Germany*
[2]*MPA/SHAO Joint Center for Astrophysical Cosmology at Shanghai Astronomical Observatory, Nandan Road 80, Shanghai 200030, China*
[3]*SUPA, Institute for Astronomy, Royal Observatory Edinburgh, Blackford Hill, Edinburgh EH9 3HJ*
[4]*Center for Astrophysical Sciences, Department of Physics and Astronomy, Johns Hopkins University, Baltimore, MD 21218, USA*

Accepted 2010 April 21. Received 2010 April 21; in original form 2009 October 19

ABSTRACT

We compute the cross-correlation between a sample of 14 000 radio-loud active galactic nuclei (RLAGN) with redshifts between 0.4 and 0.8 selected from the Sloan Digital Sky Survey and a reference sample of 1.2 million luminous red galaxies in the same redshift range. We quantify how the clustering of RLAGN depends on host galaxy mass and on radio luminosity. RLAGN are clustered more strongly on all scales than control samples of radio-quiet galaxies with the same stellar masses and redshifts, but the differences are largest on scales less than ∼1 Mpc. In addition, the clustering amplitude of the RLAGN varies significantly with radio luminosity on scales less than ∼1 Mpc. This suggests that the gaseous environment of a galaxy on the scale of its dark matter halo, plays a key role in determining not only the probability that a galaxy is RLAGN, but also the total luminosity of the radio jet. Next, we compare the clustering of radio galaxies with that of radio-loud quasars in the same redshift range. Unified models predict that both types of active nuclei should cluster in the same way. Our data show that most RLAGN are clustered more strongly than radio-loud QSOs, even when the AGN and QSO samples are matched in both black hole mass and radio luminosity. Only the most extreme RLAGN and radio-loud QSOs (RLQSOs) in our sample, with radio luminosities in excess of $\sim 10^{26}$ W Hz^{-1}, have similar clustering properties. The majority of the strongly evolving RLAGN population at redshifts ∼0.5 are found in different environments to the quasars, and hence must be triggered by a different physical mechanism.

Key words: galaxies: active – galaxies: evolution – quasars: general – radio continuum: galaxies.

1 INTRODUCTION

In recent years, interest in the radio active galactic nuclei (AGN) phenomenon among galaxy formation modellers has grown. It is hypothesized that radio AGN may regulate the star formation history and mass assembly of the most massive galaxies and black holes in the Universe (e.g. Bower et al. 2006, Croton et al. 2005). Nearby radio galaxies in clusters are observed to inject a significant amount of energy into the surrounding gas (Böhringer et al. 1993; McNamara et al. 2000; Fabian et al. 2003). As the radio jets expand and interact with the surrounding medium, they are believed to heat the gas and prevent further accretion on to the central galaxy.

The precise conditions that determine whether an AGN develops radio jets/lobes are still a matter of debate. Several studies have shown that the probability for a galaxy to become radio-loud is a strong function of stellar mass and redshift (e.g. Best et al. 2005; Donoso, Best & Kauffmann 2009). The role that the environment plays in triggering or regulating the radio-loud AGN (RLAGN) phenomenon is not as well established.

Ledlow & Owen (1996) found that the fraction of radio sources and the shape of the bivariate radio-optical luminosity function (defined as the fraction of galaxies with luminosities in the range L to $L + dL$ that have radio luminosities in the range P to $P + dP$) were the same for objects in cluster and field environments. Best et al. (2007) found that group and cluster galaxies had similar radio properties to field galaxies, but the brightest galaxies at the centres of the groups were more likely to host RLAGN than other galaxies of the same stellar mass. In the local universe, Mandelbaum et al. (2009) analyzed a large sample of RLAGN at $z \sim 0.1$. They showed that RLAGN inhabit massive dark matter haloes ($>10^{12.5}$ M$_\odot$) and that at fixed stellar mass, RLAGN are found in more massive dark matter haloes than 'control' galaxies of the same mass that are selected without regard to AGN properties. This result implies that RLAGN follow a different halo mass–stellar mass relation than normal galaxies. Mandelbaum et al. (2009) also found that the halo masses of

⋆E-mail: edonoso@mpa-garching.mpg.de

© 2010 The Authors. Journal compilation © 2010 RAS

Downloaded from http://mnras.oxfordjournals.org/ at Royal Observatory Library on November 20, 2014

RLAGN did not depend on radio luminosity. Similar results were obtained by Wake et al. (2008) who studied the clustering of low-power radio galaxies in the 2SLAQ survey (see Cannon et al. 2006). They found that radio-detected galaxies were more clustered than radio-quiet sources matched in colour and luminosity. This implied that RLAGN were located in more massive haloes than radio-quiet galaxies of the same luminosity. Hickox et al. (2009) investigated the clustering of a small sample of higher-redshift RLAGN selected from the AGN and Galaxy Evolution Survey (AGES). They found no difference in the clustering amplitude of radio galaxies and normal galaxies matched in redshift, luminosity and colour.

Most nearby RLAGN lack any of the standard accretion-related signatures; for example, strong nuclear X-ray or mid-IR emission, which would indicate that their black holes are growing significantly at the present day (see Hardcastle, Evans & Croston 2006). In contrast, quasars are believed to be powered by supermassive black holes accreting at close to the Eddington rate. Large redshift surveys, for example the Two Degree Field Galaxy Redshift Survey (2dFGRS) and the Sloan Digital Sky Survey (SDSS), now provide angular positions, accurate photometry and spectra for tens of thousands of QSOs. Recent determinations of the quasar two-point correlation function have demonstrated that at $z < 2.5$, quasars cluster like normal L_* galaxies (Croom et al. 2005; Coil et al. 2007) and populate dark matter haloes of $\sim 10^{12}\,\mathrm{M}_\odot$, with the clustering only weakly dependent on luminosity, colour and virial black hole mass (Shen et al. 2009).

As one moves out in redshift, the number density of the more powerful RLAGN increases strongly with redshift ((Dunlop & Peacock 1990). Whether the RLAGN population also evolves strongly in black hole accretion rate, is considerably less clear. In particular, we do not yet fully understand whether there is a relationship between powerful, high-redshift RLAGN and quasars. Around 10 per cent of the quasar population is radio-loud. Numerous investigations have found that radio-loud quasars and at least *some* powerful radio galaxies share a number of common characteristics, such as excess infrared emission, comparable radio morphologies and luminosities, optical emission lines, strong redshift evolution, and host galaxies with similar properties. It has thus been tempting to link both phenomena under the hypothesis that they are the same active nuclei viewed at different orientations (e.g. Barthel 1989; Urry & Padovani 1995).

A few facts are believed to be key in any attempt to understand the transition from the population of low-luminosity radio AGN produced by weakly accreting black holes at low redshifts, to a population of high-luminosity radio AGN that may be produced by strongly accreting black holes at high redshifts. Fanaroff & Riley (1974) found an important correlation between radio morphology and radio power: low-luminosity sources (Fanaroff-Riley Class I, FRI) show emission peaking close to the nuclei that fades towards the edges, whereas more luminous sources (Fanaroff-Riley Class II, FRII) are brightest towards the edges. Hine & Longair (1979) discovered that radio galaxies could also be classified according to the strength of their optical emission lines: low-excitation (weak-lined) radio galaxies or LERGs, and high-excitation (strong-lined) objects or HERGs. Modern unification models usually associate quasars with the most powerful HERGs, and low-luminosity LERGs with BL Lac objects. Although there is a notable correspondence between RLAGN luminosity, morphology and spectral type, i.e. lower-luminosity FRIs with LERGs, and higher-luminosity FRIIs with HERGs, the correlations between these properties are not straightforward. There are populations of FRI sources with high-excitation nuclear lines, and conversely, FRII galaxies with low-excitation spectra are also common. The fraction of low-luminosity FRII sources with high-excitation spectra is around 50 per cent, but this value increases to about 100 per cent for the most luminous FRII radio galaxies (Laing et al. 1994; Jackson 1999).

It has been known for years that very high redshift ($z > 2$), powerful radio galaxies are often surrounded by galaxy overdensities with sizes of a few Mpc (e.g. Pentericci et al. 2000; Miley et al. 2006). Since we know that quasars at the same redshift are clustered like normal L_* galaxies (e.g. Croom et al. 2005; Coil et al. 2007; Padmanabhan et al. 2009) and that there is little dependence on luminosity, redshift or black hole mass (e.g. Porciani & Norberg 2006; da Ângela et al. 2008; Shen et al. 2009), this would seem to throw some doubt on a simple unified scheme for explaining both phenomena.

In view of this highly complex situation, a more statistical approach to comparing the properties of quasars and radio galaxies may yield further insight. In this paper we present measurements of the projected cross-correlation between a sample of 14 000 RLAGN with a median redshift of $z = 0.55$ with the surrounding population of massive galaxies ($M_* > 10^{11}\,\mathrm{M}_\odot$). The amplitude of the cross-correlation function on large scales provides a sensitive diagnostic of the typical masses of the dark matter haloes that host the AGN, while on scales less than $\sim$1 Mpc, the correlation amplitude constrains how the AGN are distributed within these haloes (for example, whether they are usually found in central or in satellite galaxies). The large size of our samples allows us to investigate in detail how clustering depends on stellar mass and on radio luminosity. By comparing the RLAGN clustering with results from control samples matched in redshift, luminosity and mass, we isolate the effect that the radio AGN phenomenon has on the clustering signal.

We also cross-correlate radio quasars drawn from the SDSS with the same reference sample of massive galaxies. If the unified model linking radio loud quasars with RLAGN is correct, one would expect the two populations to be clustered in exactly the same way. Once again, by using control samples matched in black hole mass and radio luminosity, we ensure that we compare RLAGN and radio-loud QSOs (RLQSOs) in as uniform a way as possible.

This paper is organized as follows. In Section 2 we describe the surveys and samples used in this work. In Section 3 we explain the methodology adopted to calculate the two-point correlation function. Section 4 presents the results on RLAGN and quasar clustering. Finally, in Section 5 we summarize our results and discuss the implications of this work.

Throughout the paper we assume a flat ΛCDM cosmology, with $\Omega_m = 0.3$ and $\Omega_\Lambda = 0.7$. We adopt $h = H_0/(100\ \mathrm{km\ s^{-1}\ Mpc^{-1}})$ and present our measurements of the projected correlation function $w_\mathrm{p}(r_\mathrm{p})$, in units of Mpc h^{-1}. If h is omitted in the text, $h = 1$ is implied.

2 DATA

2.1 The MegaZ-LRG galaxy catalogue

The Sloan Digital Sky Survey (York et al. 2000; Stoughton et al. 2002) is a five-band photometric and spectroscopic survey that has mapped almost a quarter of the sky, providing precise photometry for more than 200 million objects and accurate redshifts for about a million galaxies and quasars. The MegaZ-LRG (Collister et al. 2007) is a photometric redshift catalogue based on imaging data from the fourth Data Release (DR4) of the SDSS. It consists of $\sim$1.2 million Luminous Red Galaxies (LRG) with limiting magnitude $i < 20$ over the redshift range $0.4 < z < 0.8$. MegaZ adopts various

Downloaded from http://mnras.oxfordjournals.org/ at Royal Observatory Library on November 20, 2014

colour and magnitude cuts to isolate red galaxies at $0.4 < z < 0.8$. The cuts are very similar to those adopted by the '2dF-SDSS LRG and Quasar' project (2SLAQ, Cannon et al. 2006). Accurate photometric redshifts are available for the entire LRG sample. These are derived using a neural network photometric redshift estimator (ANNz, Collister & Lahav 2004) that was trained using a sample of ∼13 000 LRGs with spectroscopic redshifts selected from 2SLAQ. The rms average photometric redshift error for all the galaxies in the sample is $\sigma_{\rm rms} = 0.049$.

Stellar masses were derived for all the galaxies in the MegaZ-LRG catalogue and the reader is referred to Donoso et al. (2009) for a detailed description of our methodology. We use the *k-correct* algorithm (Blanton & Roweis 2007), which fits a linear combination of spectral templates to the flux measurements for each galaxy. These templates are based on a set of Bruzual & Charlot (2003) models, so they can be used to estimate the mass-to-light ratio of a galaxy. This algorithm yields stellar masses that differ by less than 0.1 dex on average from estimates using other methods (for example, the method based on fitting the 4000 Å break strength and $H\delta$ absorption index proposed by Kauffmann et al. 2003).

At $z \sim 0.5$, late M-type stars have colours similar to luminous red galaxies. The Collister et al. (2007) catalogue includes a parameter $\delta_{\rm sg}$, which represents the probability that a particular object is a galaxy rather than a star. It is derived from a neural network that was trained using the 2SLAQ spectroscopic survey, and that accepts 15 different photometric parameters as input. In our analysis we only consider objects with $\delta_{\rm sg} > 0.7$. The expected contamination level by stars is then only ∼0.6 per cent (see fig. 13 of Collister et al. 2007).

2.2 The radio-loud galaxy sample

By combining the optical MegaZ-LRG catalogue with data from the NRAO VLA Sky Survey (NVSS; Condon et al. 1998) and the VLA Faint Images of the Radio Sky at Twenty Centimeters (FIRST; Becker, White & Helfand 1995), Donoso et al. (2009) constructed a catalogue of 14 453 RLAGN with 1.4 GHz fluxes above 3.5 mJy. The cross-matching method utilized a collapsing algorithm to identify multiple-component FIRST and NVSS sources and the method was optimized to take advantage of both surveys. NVSS has sufficient surface brightness sensitivity to provide accurate flux measurements of extended radio sources with lobes and jets. On the other hand, the superior angular resolution of FIRST is crucial to identify the central core component of each radio source and to provide a robust association between the radio source and the optically identified host galaxy.

Monte Carlo simulations were used to estimate the reliability (∼98.3 per cent) and completeness level (95 per cent) of the catalogue. The vast majority of the detected radio AGN (78.6 per cent) are single-component sources in both NVSS and FIRST. There is, however, a significant fraction of objects without (catalogued) high S/N FIRST detections (∼8 per cent), so the authors introduced a method for analyzing radio maps that allowed them to dig deeper into the FIRST survey and to use lower S/N detections to pinpoint the location of the host galaxy. We refer the reader to the original paper by Donoso et al. (2009) for a detailed description of these procedures and the matching algorithm.

2.3 The radio-loud and radio-quiet quasar samples

In this work we use quasars selected from the fourth edition of the SDSS spectroscopic quasar catalogue (Schneider et al. 2007). This contains 77 429 quasars drawn from SDSS DR5, with luminosities larger than $M_i = -22$, that have at least one broad emission line with FWHM > 1000 km s^{-1} in their spectra. The catalogue also identified radio-loud quasars with FIRST components within a 2-arcsec radius.

Most of the objects spectroscopically targeted as quasars were initially selected using the algorithm of Richards et al. (2002), which identifies candidates using *ugriz* broad-band photometry and by matching with unresolved FIRST sources. As the survey progressed, the quasar selection software was modified to improve its efficiency at high redshift. This is reflected in two spectroscopic target selection flags listed as TARGET and BEST (for the final algorithm). Photometry of quasars is also available in two versions, TARGET measurements (values used at the time of targeting) and BEST measurements (values derived with the latest pipeline). We note that the selection of UV-excess quasars at low redshifts ($z < 3$) has remained essentially unchanged, so that only small differences arise from using TARGET or BEST versions. The bias introduced by selection of targets using FIRST radio detections is significant only at high redshifts.

In this work we are interested in cross-correlating the quasars with the LRGs described above. We therefore selected a homogeneous sample consisting of all quasars with $0.35 < z < 0.78$ and psf magnitudes in the range $15 < i < 19.1$. We only consider primary objects (primary = 1) with point source morphology (morphology = 0), that were also targeted as primary science objects (scienceprimary = 1). This yields a sample of 7128 quasars.

Of these 7128 quasars, 684 (9.6 per cent) have radio identifications in the FIRST survey down to the 1 mJy flux density limit. One issue that could affect the derived radio luminosities of the QSOs in our sample is that a fraction of them present a truly extended FRII-like morphology, and the total radio flux is distributed over many components. The exclusion of such structures might result in the total radio luminosity being underestimated. We visually examined NVSS/FIRST radio maps of the 678 QSOs with FIRST detections and added the NVSS fluxes of the associated component(s), if present, or of the FIRST component(s) when no NVSS source was found nearby. The derived radio luminosities increase by a factor of ∼2–3 for some QSOs. We note that we repeated the clustering analysis described in Section 4.2 using only the central (core) component fluxes, and we verified that this has no significant influence on any of our results.

It is conventional to identify radio-loud quasars by means of the ratio of flux in the radio to that in the ultraviolet (e.g. Kellerman et al. (1989), Stocke et al. (1992)). We have chosen to define radio-loud quasars as those with total integrated 1.4-GHz radio power (after adding all associated components) above 10^{25} W Hz^{-1}. This definition is independent of the UV/optical luminosity of the quasar and ensures that our sample is comparable in its distribution of radio luminosities to the RLAGN that lie above the 'break' in the radio luminosity function. With this definition, there are 307 radio-loud quasars in our sample. Objects below this luminosity (or non-detections) are considered to be radio-quiet quasars.

2.4 Sample properties

Shen et al. (2008) have derived virial black hole mass estimates for SDSS DR5 quasars. These are based on Hβ, MgII and CIV emission lines, and the continuum luminosities around these lines. We adopt these estimates for our quasar sample (at $z < 0.7$, these are mostly derived from Hβ). For RLAGN we adopted the relation between black hole mass and bulge mass derived by Häring & Rix

Downloaded from http://mnras.oxfordjournals.org/ at Royal Observatory Library on November 20, 2014

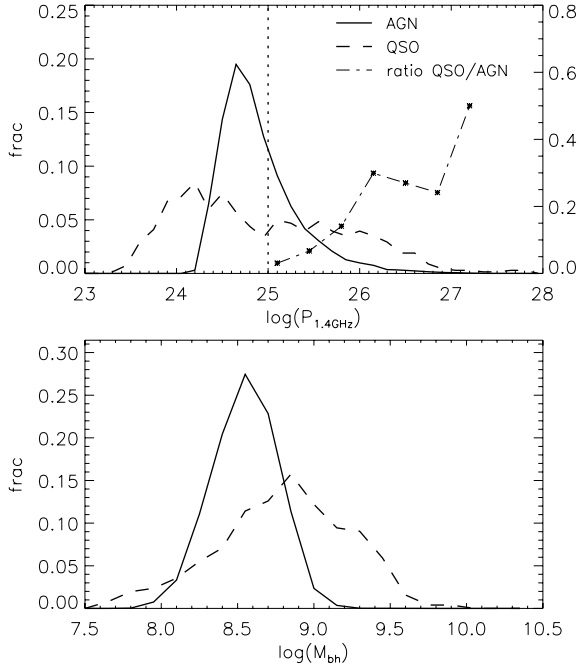

Figure 1. Top: Normalized distribution of radio luminosity ($P_{1.4\,\mathrm{GHz}}$) corresponding to radio-loud AGNs (solid), and to QSOs detected down to 1 mJy in the FIRST survey (dashed). The vertical line at 10^{25} W Hz^{-1} marks the adopted threshold between radio-quiet and radio-loud QSOs. Also shown is the ratio of the number of radio-loud quasars relative to radio AGN (scale on the right axis). Bottom: Distribution of black hole mass (M_{bh}) for radio-loud AGNs and radio-loud QSOs.

(2004), $M_{\mathrm{bh}} = 0.0014 M_{\mathrm{bulge}}$, where we replace M_{bulge} by the stellar mass of the galaxy. At the lower end of our galaxy mass distribution ($\sim 10^{11}$ M$_\odot$), use of the stellar mass instead of the bulge mass may cause the black hole mass to be overestimated by a factor of $\sim$1.2–1.4. We note that the majority of RLAGN in our sample are more massive than this.

For reference, Fig. 1 shows the radio luminosity and black hole mass distributions derived for all the RLAGN and radio-loud QSO in our samples. In the upper panel, we also plot the ratio of the number of RLQSOs to RLAGN and show that this increases from $\sim$1 per cent at 10^{25} W Hz^{-1} up to $\sim$50 per cent at 10^{27} W Hz^{-1}. At the very highest radio luminosities, our results are broadly consistent with Lawrence (1991) who found similar ratios of broad-lined and narrow-lined 3CR sources.

One variation of the unified model that has been introduced to explain the trend in the relative numbers of RLQSO and RLAGN is the so-called receding torus model (e.g. Simpson 1998), in which the inner radius of the obscuring torus (which is identified with the dust sublimation radius) scales with luminosity as $L^{0.5}$. This model can obviously only apply at the highest radio luminosities, where the numbers of RLQSO and RLAGN are comparable.

3 CLUSTERING ANALYSIS

3.1 The cross-correlation function

A standard way to characterize the clustering of galaxies is with the two-point correlation function $\xi(r)$, which measures the excess in the number of pairs of objects with separation r in a volume dV, with respect to a random distribution with the same mean number density of objects n (Peebles 1980). This can be expressed as

$$dP = n^2[1 + \xi(r)]dV^2. \quad (1)$$

Objects are said to be clustered if $\xi > 0$. The amplitude and shape of the correlation function yield a variety of different information. On scales larger than a few Mpc, the amplitude is a measure of the mass of dark matter haloes in which the galaxies are found (e.g. Sheth & Tormen 1999). On intermediate scales, the shape of the correlation function is sensitive to how galaxies are distributed within their haloes (Li et al. 2006b), while at scales smaller than a few hundred kpc it probes processes such as mergers or interactions (Li et al. 2008).

Several estimators for the (auto)correlation function have been proposed in the literature. In this work we calculate the autocorrelation function of the LRGs using the estimator of Hamilton (1993),

$$\xi(r) = \frac{DD(r)RR(r)}{[DR(r)]^2} - 1, \quad (2)$$

where $DD(r)$, $RR(r)$ and $DR(r)$ respectively refer to the normalized number of (LRG–LRG), (random–random) and (LRG–random) pairs as a function of the spatial separation r (see the next section for details about the construction of the random sample).

To estimate the cross-correlation function of RLAGN or quasars with the MegaZ-LRG galaxy sample, we count the number of LRGs around each AGN or quasar as a function of distance, and divide by the expected number of pairs for a random distribution,

$$\xi(r) = \frac{CD(r)}{CR(r)} - 1, \quad (3)$$

where $CD(r)$ stands for the number of (RLAGN/QSO-LRG) pairs, $CR(r)$ is the number of (RLAGN/QSO-random) pairs and the quantities have been normalized by the number of objects in the LRG and random catalogues. The advantage of our procedure is that it does not require full knowledge of the QSO or RLAGN selection function. Only the LRG selection function is needed for the construction of the random sample, and this is well quantified. Another reason for calculating cross-correlations rather than autocorrelations, is that it allows us to overcome shot noise when the sample size is small. We note that the LRG sample (D in the notation above) remains fixed throughout this work. The error bars of the auto- and cross-correlation functions are calculated via statistical bootstrapping by drawing 100 random samples with replacement.

In practice, photometric redshift errors as well as distortions due to peculiar velocities along the line of sight will introduce systematic effects in our estimate of $\xi(r)$. Therefore, to recover real-space clustering properties we decompose ξ in two directions, along the line of sight (π) and perpendicular to it (r_{p}). Integrating over the π-direction allows to define the projected two-point cross-correlation function $w_{\mathrm{p}}(r_{\mathrm{p}})$, a quantity that is independent of such distortions (Davis & Peebles 1983). A detailed description of the method can be found in Li et al. (2006b).

It should be noted that at $z = 0.55$, the rms photometric redshift error corresponds to an error in the distance between two galaxies of $\sim\pm$160 Mpc h^{-1}. The photometric redshift error distributions are well approximated by a Gaussian (albeit with somewhat wider wings). To derive $w_{\mathrm{p}}(r_{\mathrm{p}})$, we therefore integrate along the π-direction over the range $-$200 Mpc h^{-1} to $+$200 Mpc h^{-1}. Table 1 lists our measurements of the auto- and cross-correlations of LRGs, RLAGN, quasars, and radio-loud quasars presented in this paper.

Downloaded from http://mnras.oxfordjournals.org/ at Royal Observatory Library on November 20, 2014

Table 1. Measurements of the projected LRG–LRG autocorrelation function and the cross-correlation between RLAGN, QSO or RLQSO, and the LRG sample (see Section 4 for the definition of the samples).

r_p (Mpc h^{-1})	LRG–LRG	RLAGN–LRG					QSO–LRG	RLQSO–LRG
		Total	$M < 11.3$	$M > 11.6$	$P < 24.6$	$P > 25.7$		
1	2	3	4	5	6	7	8	9
0.032	3491 ± 144	7276 ± 904	6414 ± 1892	8800 ± 2241	7389 ± 2289	6266 ± 1816	1907 ± 993	-
0.051	2497 ± 88	5912 ± 577	4933 ± 1068	8904 ± 1681	5822 ± 1295	2423 ± 594	1527 ± 504	-
0.081	1632 ± 48	4496 ± 349	2660 ± 516	6086 ± 769	3671 ± 638	3440 ± 645	909 ± 283	1133 ± 797
0.129	1021 ± 25	2567 ± 164	1969 ± 290	3311 ± 392	2359 ± 312	2016 ± 251	645 ± 197	1228 ± 923
0.204	655 ± 12	1529 ± 96	1286 ± 175	1833 ± 182	1425 ± 195	1060 ± 147	266 ± 74	550 ± 298
0.324	398 ± 7.3	896 ± 45	731 ± 74	1268 ± 109	781 ± 88	673 ± 90	298 ± 58	292 ± 154
0.514	241 ± 4.1	506 ± 22	371 ± 45	709 ± 55	485 ± 52	422 ± 50	103 ± 34	98.7 ± 68
0.815	144 ± 2.3	255 ± 13	182 ± 27	337 ± 33	257 ± 29	205 ± 27	63.9 ± 18	132 ± 64
1.29	96.0 ± 1.6	139 ± 8.5	107 ± 17	182 ± 19	162 ± 19	121 ± 17	58.0 ± 13	47.9 ± 38
2.04	65.9 ± 1.1	96.1 ± 6.3	73.7 ± 11	118 ± 11	105 ± 14	102 ± 11	37.6 ± 9.3	54.8 ± 23
3.24	47.3 ± 1.0	69.1 ± 5.5	61.2 ± 9.6	82.3 ± 9.4	82.2 ± 12	56.9 ± 9.1	28.2 ± 8.1	19.6 ± 15
5.14	32.7 ± 0.7	45.6 ± 4.2	34.9 ± 8.5	56.1 ± 7.6	49.1 ± 9.3	39.5 ± 8.0	23.3 ± 7.3	19.5 ± 13
8.15	22.5 ± 0.7	31.7 ± 3.8	29.4 ± 7.8	36.2 ± 6.9	33.5 ± 9.0	32.2 ± 7.2	15.8 ± 6.5	7.3 ± 13
12.9	14.5 ± 0.6	20.4 ± 3.9	18.5 ± 7.4	23.9 ± 6.8	21.6 ± 8.5	17.7 ± 7.0	9.6 ± 6.2	5.9 ± 12
20.4	8.7 ± 0.6	12.3 ± 3.6	10.3 ± 6.7	15.7 ± 6.3	14.0 ± 8.1	11.3 ± 6.5	4.9 ± 6.0	4.9 ± 11
32.4	4.4 ± 0.6	6.7 ± 3.4	7.0 ± 6.6	6.7 ± 6.2	7.9 ± 8.1	10.4 ± 6.6	2.8 ± 5.8	3.4 ± 11

3.2 Construction of the random sample

The random sample used in estimating the cross-correlation function should have the same selection effects as the observed galaxies. We follow the method by Li et al. (2006a): we take observed LRG sample that fall within the coverage mask of SDSS DR4 and randomly re-assign the sky coordinates of each galaxy. All other quantities such as redshift, stellar mass and luminosity are kept fixed. Because the survey covers a very wide area (>6000 deg^2 for SDSS DR4), this procedure is sufficient to remove any coherence in the radial direction and it ensures that the geometry of the random catalogues is exactly the same as the real one, and that all redshift-dependent selection effects are accounted for. We generate 10 random samples in this way.

4 RESULTS

4.1 Radio-loud AGN clustering

It is well known that the clustering amplitude of galaxies varies as a function of mass, luminosity and redshift. Radio AGN are usually hosted by very massive, $>3L_*$ galaxies (Best et al. 2005; Donoso et al. 2009). To take this into account, we select control samples of radio-quiet MegaZ-LRG galaxies with redshifts, stellar masses and absolute magnitudes that closely match the radio AGN sample. For each RLAGN we randomly select 10 radio-quiet LRG (or five, depending on the number of available candidates) within a tolerance of $\Delta z = 0.02$ in redshift, $\Delta M = 0.1$ in log stellar mass and $\Delta M_i = 0.05$ in absolute magnitude, where M_i is the extinction and k-corrected i-band absolute magnitude of the galaxy. Fig. 2 shows the distributions of these parameters for radio-loud, radio-quiet and control objects.

Using the methods described in the previous section, we first calculate the autocorrelation function for our reference sample of luminous red galaxies. We then cross-correlate the RLAGN with the LRG parent sample. This is shown in Fig. 3, where it can be seen that RLAGN are significantly more clustered than the LRG population on all spatial scales. The two main contributions to the clustering signal, which arise from galaxies within the same halo

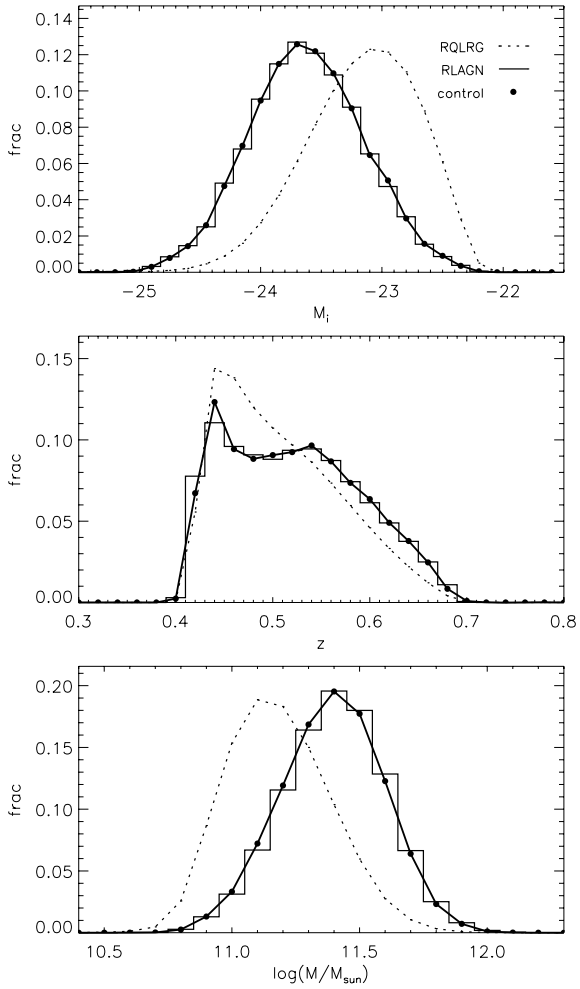

Figure 2. Normalized distributions of i-band absolute magnitude, redshift and stellar mass for radio-quiet LRGs (dotted), radio-loud AGN (histogram), and control radio-quiet LRGs (large dots).

Downloaded from http://mnras.oxfordjournals.org/ at Royal Observatory Library on November 20, 2014

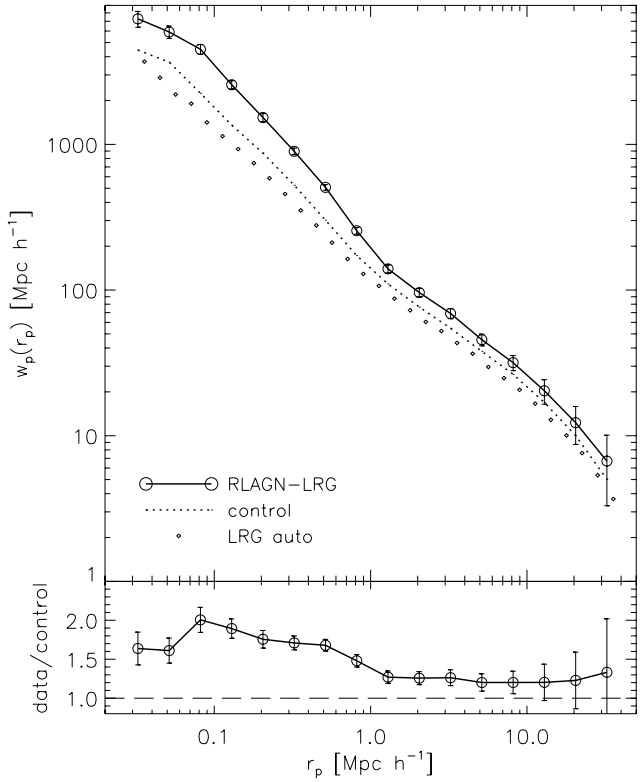

Figure 3. Projected cross-correlation function $w_p(r_p)$ between radio-loud AGN and MegaZ luminous red galaxies (solid) in the range 0.03–30 Mpc h^{-1}. The LRG–LRG autocorrelation is indicated by small diamond symbols. Also shown is the cross-correlation of a control sample of radio-quiet LRG (dashed) with the same distribution of redshifts, luminosities and stellar masses as the radio-loud population. The bottom panel shows the ratio of $w_p(r_p)$ for the RLAGN to that for the control sample. Note that the errors in the LRG autocorrelation and the control galaxy cross-correlation functions are very small, so we have omitted them in this and subsequent plots.

and from galaxies in different haloes, are clearly visible, with the transition occurring around 1 Mpc h^{-1}. The difference in the clustering amplitude between RLAGN and normal LRGs is strongest on scales less than 1 Mpc h^{-1}. This tells us that RLAGN and control galaxies must be distributed in different ways within their dark matter haloes. We intend to model this in more detail in upcoming work.

If we compare the clustering of RLAGN with that of control galaxies with the same redshifts, luminosities and stellar masses, we see that RLAGN are still significantly more clustered. The bottom panel shows the ratio between $w_p(r_p)$ for the RLAGN and the control galaxies; we call this the *relative bias* of the RLAGN sample. This plot demonstrates that the probability for a galaxy to be radio-loud depends on environment as well as on galaxy or black hole mass. In Table 2, we list our relative bias measurements averaged over two different spatial scales ($0.1 < r_p < 0.8$ and $1 < r_p < 20$ Mpc h^{-1}). Results are given for all the RLAGN and quasar samples analyzed in the following sections.

4.1.1 Dependence on stellar mass

We split the RLAGN sample into two subsamples with $\log(M/M_\odot) < 11.3$ and with $\log(M/M_\odot) > 11.6$. We also applied the same split to the corresponding control samples. The resulting cross-correlations are plotted in Fig. 4. As expected, more massive radio galaxies are more strongly clustered on all scales. When compared to control galaxies, both subsamples show roughly the same relative clustering strength on scales larger than 1–2 Mpc h^{-1}. On small scales the difference between control and data samples is larger for RLAGN in less massive galaxies. These results are in good agreement with those of Mandelbaum et al. (2009) for RLAGN at lower redshifts.

We now investigate how the clustering of RLAGN and their control galaxies varies *as a function* of stellar mass. We fit two power laws of the form $w(r_p) = A\, r_p^{(1-\gamma)}$ to the cross-correlation function, one over the range $0.1 < r_p < 0.8$ Mpc h^{-1} and the other over the range $1 < r_p < 20$ Mpc h^{-1}. This division allows us to quantify the clustering signal contributed by LRGs that are in the same halo as the RLAGN and by LRGs that reside in different haloes. For the complete RLAGN sample, the best-fitting parameters are $A = 233.9 \pm 15$ and $\gamma = 2.18 \pm 0.05$ on scales less than 1 Mpc h^{-1}, and $A = 173.2 \pm 10$ and $\gamma = 1.81 \pm 0.05$ on larger scales. The 1σ errors quoted on these parameters are derived from the covariance matrix of the least-squares regression coefficients used in the fit.

We then divide the sample into eight mass bins and perform new fits, keeping the slope of the power law fixed, but allowing the normalization to vary. Fig. 5 shows the cross-correlation amplitudes as a function of stellar mass for RLAGN, and for the radio-quiet control sample. As can be seen, the ratio between the clustering amplitude of the RLAGN and the control galaxies depends both on stellar mass and on the scale at which the clustering is evaluated. On scales less than 1 Mpc h^{-1}, there is a relatively strong dependence of the ratio on stellar mass, with RLAGN in low-mass galaxies clustered much more strongly than the controls, but RLAGN in high-mass galaxies clustered similarly to the controls. On larger scales, there is a much weaker trend in the ratio with mass.

Table 2. Mean clustering bias of RLAGN (relative to the respective control sample) and of RLQSO (relative to the LRG autocorrelation function). Error bars are calculated via statistical bootstrapping.

Sample	$0.1 < r_p < 0.8$ Mpc h^{-1}	$1 < r_p < 20$ Mpc h^{-1}
Total RLAGN	1.75 ± 0.10	1.23 ± 0.12
RLAGN $\log(M/M_\odot) < 11.3$	2.09 ± 0.28	1.19 ± 0.29
RLAGN $\log(M/M_\odot) > 11.6$	1.39 ± 0.13	1.16 ± 0.23
RLAGN $\log(P_{1.4\,\mathrm{GHz}}) < 24.6$	1.57 ± 0.20	1.36 ± 0.29
RLAGN $\log(P_{1.4\,\mathrm{GHz}}) > 25.7$	1.46 ± 0.22	1.13 ± 0.35
Total QSO	0.53 ± 0.14	0.63 ± 0.29
RLQSO ($\log(P_{1.4\,\mathrm{GHz}}) > 25$)	0.79 ± 0.50	0.51 ± 0.47
RLAGN ($\log(P_{1.4\,\mathrm{GHz}}) > 25$)	2.43 ± 0.22	1.38 ± 0.21
Control RLAGN matched in $M_{bh}/P_{1.4\,\mathrm{GHz}}$	2.27 ± 0.42	1.39 ± 0.56
Control RLAGN matched in $P_{1.4\,\mathrm{GHz}}$	1.97 ± 0.38	1.37 ± 0.57

4.1.2 Dependence on radio luminosity

We now investigate if there is any dependence of RLAGN clustering on the luminosity of the radio source. Prestage & Peacock (1988) studied the local galaxy density around radio galaxies at $z < 0.25$, and found that weak FRI sources were in denser regions than the more luminous FRII sources. Yates, Miller & Peacock (1989) (and later Hill & Lilly 1991) extended such studies to higher redshifts and concluded that powerful radio galaxies at $z \sim 0.5$ are typically

Downloaded from http://mnras.oxfordjournals.org/ at Royal Observatory Library on November 20, 2014

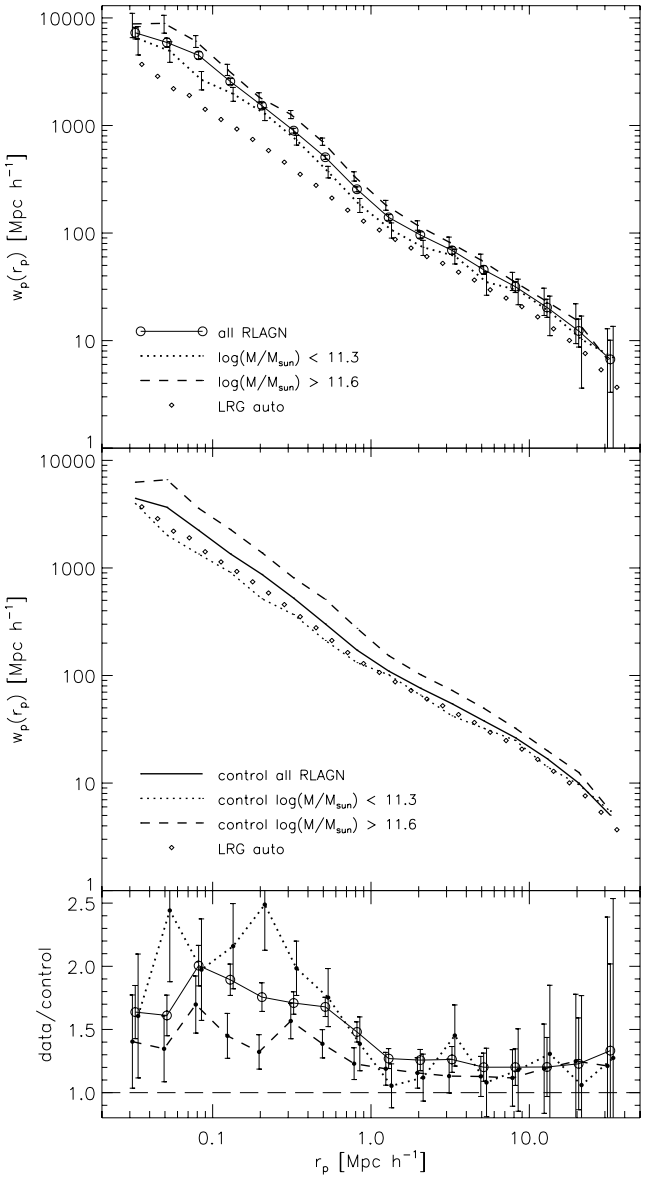

Figure 4. Top: Projected cross-correlation function $w_p(r_p)$ between radio-loud AGN and MegaZ luminous red galaxies (solid) in the range 0.03–30 Mpc h^{-1}. The dashed and dotted lines indicate the cross-correlation of massive objects with $\log(M/M_\odot) > 11.6$, and of less massive systems with $\log(M/M_\odot) < 11.3$. The LRG–LRG autocorrelation function is shown for reference (diamond symbols). Middle: Cross-correlation of control samples of radio-quiet LRGs that have the same distribution of redshift and stellar mass as the radio-loud systems. Bottom: Ratio of $w_p(r_p)$ between RLAGN and their corresponding control samples. Note that the curves are slightly shifted along the x-axis to improve clarity.

found in environments three times richer than their counterparts at $z \sim 0.2$. They also found that the most luminous objects were in richer environments than the less luminous ones. Given the limitations of the available samples, they were unable to determine whether the primary factors influencing the clustering trends were redshift or radio luminosity, or a combination of both. Best (2004) studied the density of galaxies around nearby RLAGN. He found a positive correlation between local density and radio luminosity for RLAGN without emission lines, but found that RLAGN with emission lines avoided high-density regions.

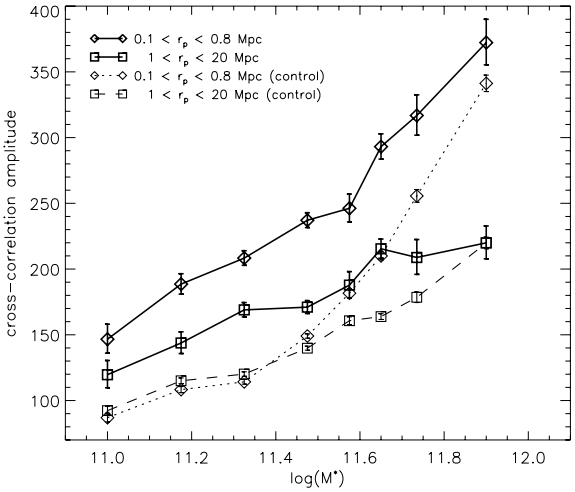

Figure 5. The dependence of the cross-correlation amplitude of RLAGN and control galaxies on stellar mass. The amplitude is computed by fitting a power law with fixed exponent (see text for details). Results are shown for RLAGN (solid lines) and their corresponding control radio-quiet LRG (dotted, dashed lines). Fits are calculated at two different spatial scales, $0.1 < r_p < 0.8$ Mpc h^{-1} and $1 < r_p < 20$ Mpc h^{-1}.

In this study, we split our RLAGN sample into a low-luminosity subsample with $\log(P_{1.4\,\mathrm{GHz}}[\mathrm{W\,Hz^{-1}}]) < 24.6$, and a high-luminosity subsample $\log(P_{1.4\,\mathrm{GHz}}[\mathrm{W\,Hz^{-1}}]) > 25.7$. These cuts allow us to sample the faint and bright end of the radio luminosity function. We build control samples in the same way as before and we present the cross-correlation results in Fig. 6. The top panel of Fig. 6 shows that low-luminosity RLAGN are more clustered than high-luminosity systems on all scales.

To quantify the variation of clustering with radio luminosity in more detail, we once again proceed by fitting a power law to the cross-correlation functions for RLAGN subsamples split by radio luminosity. We fit separate power laws on scales below and above 1 Mpc h^{-1}. The variation in the clustering amplitude with luminosity is plotted in Fig. 7. Two interesting features can be observed. First, the clustering amplitude of radio galaxies on large scales is only very weakly anti-correlated with radio power. On small scales, the clustering *increases* with radio luminosity, peaks at $\log(P_{1.4\,\mathrm{GHz}}[\mathrm{W\,Hz^{-1}}]) \sim 25.3$ and then decreases for most luminous radio sources.

Barthel & Arnaud (1996) argue that the confining effect of a dense intracluster medium reduces the adiabatic losses of radio lobes, leading to higher levels of synchrotron emission. Thus, a dense environment may provide a more effective 'working surface' for the lobes, giving rise to the positive correlation between small-scale clustering amplitude and radio luminosity observed in Fig. 7 for sources with $\log(P_{1.4\,\mathrm{GHz}}[\mathrm{W\,Hz^{-1}}]) < 25.3$. Alternatively, the correlation between clustering strength and radio luminosity may simply reflect a correlation between jet power and the local cooling rate of hot gas, which will be higher in denser regions.

Why does the clustering amplitude drop for radio sources with luminosities higher than $10^{25.3}$ $\mathrm{W\,Hz^{-1}}$? As we will argue in the next section, this radio luminosity may mark the beginning of a transition to a population of AGN that are more similar to the quasars. As we will show, quasars are significantly less clustered than most RLAGN.

Downloaded from http://mnras.oxfordjournals.org/ at Royal Observatory Library on November 20, 2014

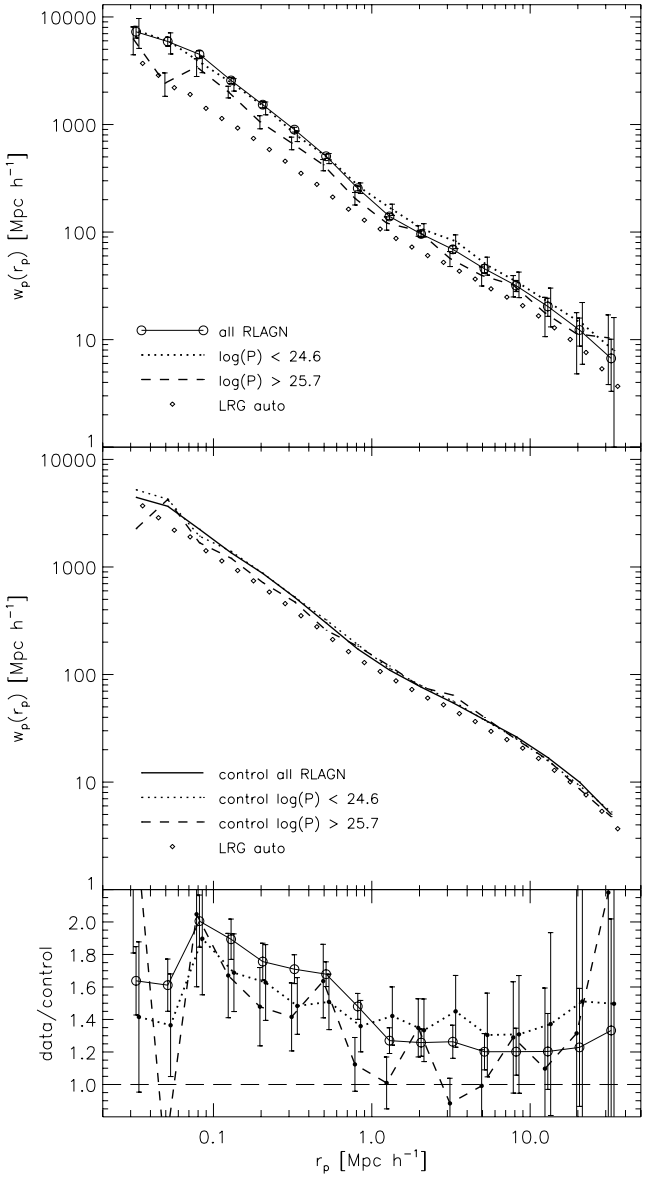

Figure 6. Top: Projected cross-correlation function $w_p(r_p)$ between radio-loud AGN and MegaZ luminous red galaxies (solid) in the range 0.03–30 Mpc h^{-1}. Dashed and dotted lines indicate the cross-correlation of luminous objects with $\log(P_{1.4\,\mathrm{GHz}}[\mathrm{W\,Hz^{-1}}]) > 25.7$, and of less powerful AGN with $\log(P_{1.4\,\mathrm{GHz}}[\mathrm{W\,Hz^{-1}}]) < 24.6$. The LRG–LRG autocorrelation is shown for reference (diamond symbols). Middle: Cross-correlation of control samples of radio-quiet LRGs that have the same distribution of redshift and stellar mass as the radio-loud systems. Bottom: Ratio of $w_p(r_p)$ between RLAGN and their corresponding control samples. Note that the curves are slightly shifted along the x-axis to improve the visibility.

4.2 Quasar clustering and AGN unification

In this section, we compare the clustering of radio galaxies and quasars at $z \sim 0.5$. Our goal is to develop a better understanding of the relationship between these two types of active galaxy.

AGN unification models provide an appealing way to account for the diversity of the observed AGN population. The basic hypothesis is that the observed characteristics of AGN depend mainly on their orientation relative to the line of sight. Comprehensive reviews of unification models can be found in Barthel (1989), Antonucci (1993) and Urry & Padovani (1995).

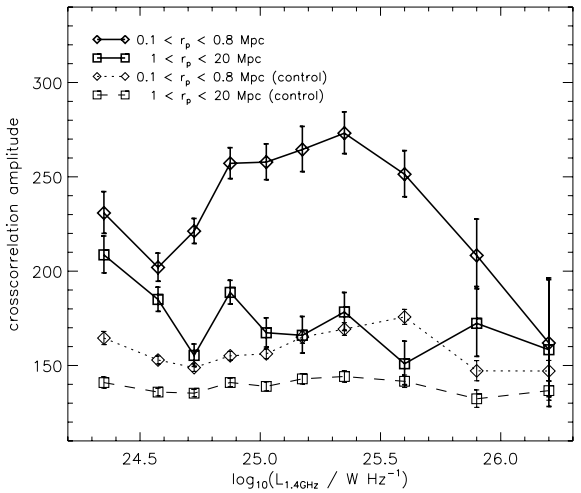

Figure 7. The dependence of the cross-correlation amplitude on radio luminosity. Results are shown for both, RLAGN (solid lines) and their corresponding control radio-quiet LRGs (dotted, dashed lines). Fits are calculated for two different ranges in scale: $0.1 < r_p < 0.8$ Mpc h^{-1} and $1 < r_p < 20$ Mpc h^{-1}.

In this paper, we attempt to test one fundamental requirement of the unification scheme of radio-loud objects, namely that the environment of radio galaxies and radio quasars should be statistically identical. We note that previous works have already suggested that low-excitation radio galaxies (which include most FRI sources, but also a significant fraction low-luminosity FRII radio galaxies) do not participate in the same unification framework as quasars or broad-line radio galaxies (e.g. Hardcastle 2004; Hardcastle, Evans & Croston 2007). We will therefore confine our attention to the most luminous radio-loud galaxies and radio-loud quasars in our sample, i.e. those with luminosities in excess of 10^{25} W $\mathrm{Hz^{-1}}$.

Up to now, observational evidence has not yielded conclusive evidence as to whether powerful RLAGN and RLQSOs cluster in the same way. The first problem is that the available samples have been small. In the local universe, powerful radio galaxies with $\log(P_{1.4\,\mathrm{GHz}}[\mathrm{W\,Hz^{-1}}]) \sim 26$ have typical comoving densities of 10^{-8} $\mathrm{Mpc^{-3}\,dex^{-1}}$ at $z \sim 0.1$, so large volumes are required to detect a significant number of sources. Smith & Heckman (1990) studied the environments of ∼30 low-redshift radio quasars and powerful radio galaxies, concluding that both populations were clustered in much the same way as radio-quiet QSOs. At higher redshifts ($0.3 < z < 0.5$), Yates et al. (1989) also found that the environments of radio galaxies and radio-loud quasars were similar, with higher-luminosity systems slightly more clustered. Barr et al. (2003) found that luminous radio-loud quasars exist in a variety of environments including rich clusters, compact groups and in low-density environments.

In this work we calculate the cross-correlation function between radio-quiet and radio-loud quasars, and the same reference sample of LRGs used in Section 4.1. The resulting $w_p(r_p)$ are plotted in Fig. 8. As can be seen, *there is no significant difference in clustering strength between radio-loud and radio-quiet quasars*. It is interesting that the clustering strength of RLAGN seems to be larger than that of radio-loud quasars on all scales, and particularly at $r_p < 1$ Mpc h^{-1}.

We note that our quasar/LRG cross-correlation function agrees quite well with that derived by Padmanabhan et al. (2009). Shen et al. (2009) analyzed the clustering of radio-loud and radio-quiet quasars in SDSS DR5 at $0.4 < z < 2.5$ and found that radio quasars

Downloaded from http://mnras.oxfordjournals.org/ at Royal Observatory Library on November 20, 2014

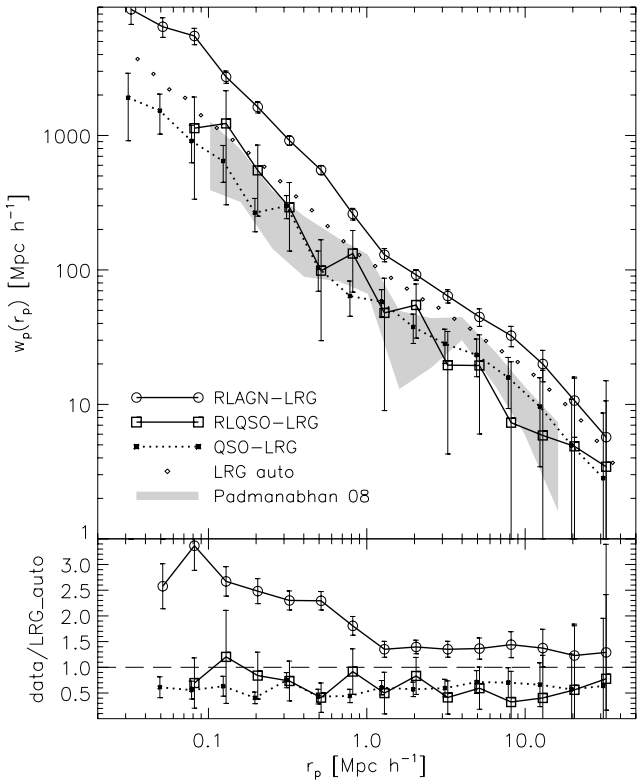

Figure 8. Projected cross-correlation function $w_p(r_p)$ between quasars and LRGs (dotted), and between radio-loud quasars and LRGs (solid, squares). For comparison, we plot the cross-correlation of radio-loud AGN and LRGs (solid, circles), as well as the LRG–LRG autocorrelation (small diamonds). The grey shaded area indicates the QSO–LRG cross-correlation derived by Padmanabhan et al. (2009). The bottom panel shows the ratio of $w_p(r_p)$ with respect to the LRG autocorrelation. The analysis is restricted to sources with integrated luminosities above 10^{25} W Hz^{-1}.

cluster more strongly than radio-quiet quasars with the same black hole masses. Our results do not appear to agree with this. As we will show in Section 4.2.1., matching the radio-quiet and radio-loud quasar sample in black hole mass does not alter our conclusion. We speculate that disagreement with Shen et al. (2009) may arise because we consider a much narrower range in redshift. We note that Wold et al. (2000) also found little difference between the environments of radio-loud and radio-quiet quasars over roughly the same redshift range as that probed in this study.

We conclude, therefore, that powerful radio galaxies appear to be hosted by very massive haloes, more massive than their quasar counterparts. In the next two subsections we will show that the clustering differences between RLAGN and RLQSOs persist, even if the samples are matched both in radio luminosity and in black hole mass. In principle, this suggests that the unification scheme for the two classes of AGN is not as straightforward as was first thought, and parameters other than orientation are required to explain the differences between RLAGN and RLQSOs.

4.2.1 Black hole mass

Some observational evidence supports the idea that radio jet power might be closely related to the mass of the black hole and its accretion rate. Links between radio luminosity and black hole mass have been found in radio galaxies (Franceschini, Vercellone & Fabian 1998) and in quasars (Lacy et al. 2001; Boroson 2002). However,

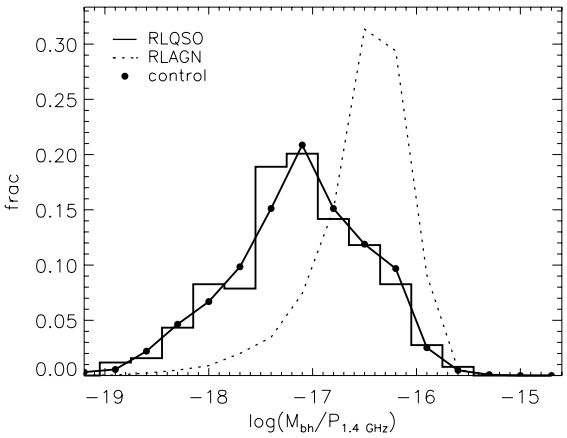

Figure 9. Normalized distributions of $M_{bh}/P_{1.4\,GHz}$ for radio-loud AGN (dotted), radio-loud QSOs (histogram) and control radio AGN (large dots) selected to have a similar distribution in $M_{bh}/P_{1.4\,GHz}$ as the radio-loud quasars.

other authors have argued against such strong correlations (Ho 2002; Snellen et al. 2003; Metcalf & Magliocchetti 2006).

To control for the effect of black hole mass, we constructed a sample of RLAGN with a similar distribution in $M_{bh}/P_{1.4\,GHz}$ as that of radio-loud quasars. The parameter $M_{bh}/P_{1.4\,GHz}$ can be considered not only as an indicator of mass, but also as a kind of inverse Eddington ratio that measures how much radio emission per unit black hole mass is produced by the jet. In the local universe, Kauffmann et al. (2008) found that RLAGN show a significant correlation between radio and emission-line (OIII) luminosity, provided both are scaled by black hole mass. As discussed by Heckman et al. (2004), galaxies with low-mass black holes are currently building up their black hole mass at a higher rate than high-mass systems. Fig. 9 shows the distribution in $M_{bh}/P_{1.4\,GHz}$ of the RLAGN and RLQSO samples before and after the matching procedure. Fig. 10 shows the resulting cross-correlations. The main result here is that matching in $M_{bh}/P_{1.4\,GHz}$ does not change the correlation function, and so the clustering differences between RLAGNs and RLQSOs persist.

From Fig. 1 it can be seen that some radio-loud quasars are hosted by black holes more massive than $10^{9.3}\,M_\odot$, which are not present in the RLAGN population (we suspect that errors in the virial black hole mass estimates are to blame). We have repeated the cross-correlation analysis of radio quasars with black hole masses in the range $10^8\,M_\odot < M_{bh} < 10^9\,M_\odot$ and find that this makes no difference to our results. Repeating the analysis by matching in black hole mass alone also does not change our conclusions.

4.2.2 Radio luminosity

It is also interesting to investigate whether clustering differences between RLAGN and quasars depend on radio luminosity. To test this, we build control samples using the same methodology as before, but this time matching in $\log(P_{1.4\,GHz})$.[1] Figs 11 and 12 show

[1] We note that a fraction of the RLQSOs will be core-dominated, so that a fraction of the luminosity of some sources will be due to beaming. This would affect the matching in radio luminosity between beamed and non-beamed objects. However, because of the weak dependence of clustering amplitude on radio luminosity for the quasars, this effect does not influence our conclusions.

Downloaded from http://mnras.oxfordjournals.org/ at Royal Observatory Library on November 20, 2014

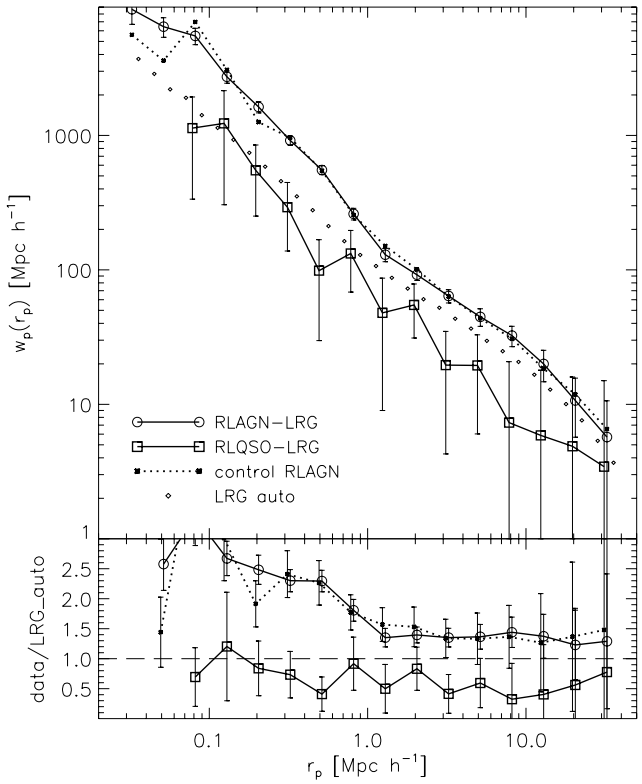

Figure 10. Projected cross-correlation function $w_p(r_p)$ between radio-loud quasars and LRGs (solid, squares). Also shown is the cross-correlation of a control sample of radio-loud AGN (dotted) selected to have a similar distribution of $M_{bh}/P_{1.4\,GHz}$ as the radio-loud quasars. For comparison, we plot the cross-correlation of RLAGN and LRG (solid, circles), and the LRG–LRG autocorrelation (small diamonds). The bottom panel shows the ratio of $w_p(r_p)$ to the LRG autocorrelation. The analysis is restricted to sources with integrated luminosities above 10^{25} W Hz^{-1}.

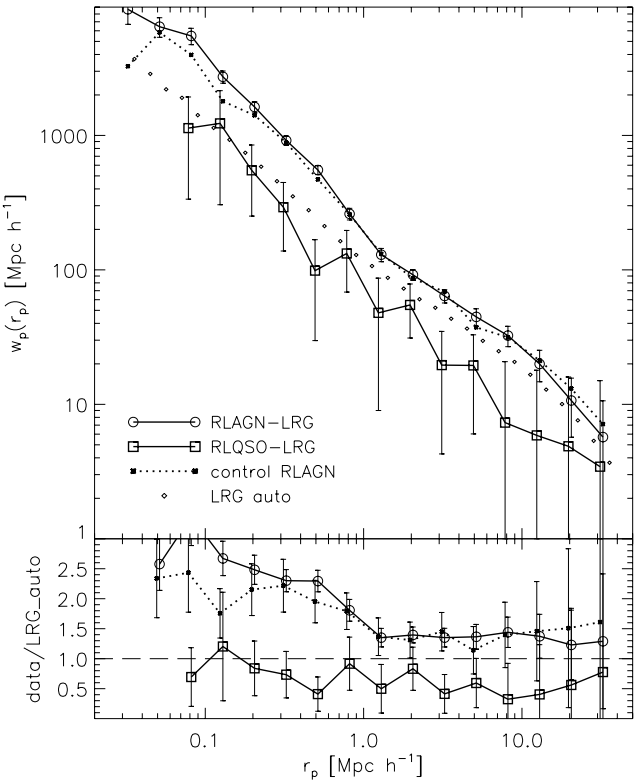

Figure 11. Projected cross-correlation function $w_p(r_p)$ between radio-loud quasars and LRG (solid, squares). Also shown is the cross-correlation of a control sample of radio-loud LRG (dotted) selected to have a similar distribution of $\log(P_{1.4\,GHz})$ as in radio quasars. For comparison we plot again cross-correlation of RLAGN and LRG (solid, circles), and the LRG–LRG autocorrelation (small diamonds). The bottom panel shows the ratio of $w_p(r_p)$ with respect to the LRG autocorrelation. The analysis is restricted to sources with integrated luminosities (after adding all associated components) above 10^{25} W Hz^{-1}.

the corresponding cross-correlation functions and radio luminosity distributions of the matched samples. The clustering of RLAGN remains essentially unchanged.

We now calculate cross-correlation functions for radio-loud quasars of increasing radio luminosities [$\log(P_{1.4\,GHz}) > 25.0$, > 25.5, > 25.75]. We find a slight increase in clustering strength as a function of radio power on all scales in the range $0.1 < r_p < 20$ Mpc h^{-1}. This is plotted in Fig. 13, where we compare the cross-correlation amplitudes of RLAGN and QSOs. The amplitude is calculated using a single power-law fit over the entire range, since the correlation function of quasars does not exhibit a clear break on a scale of $\sim$1 Mpc h^{-1}, as is the case for radio galaxies. We find that RLAGN are more strongly clustered than RLQSO in all radio luminosities that we are able to probe. However, the clustering of RLAGNs decreases strongly with luminosity above $10^{25.5}$ W Hz^{-1}. Extrapolation of our results suggests that both kinds of AGN *might* have similar clustering at radio luminosities in excess of 10^{26} W Hz^{-1}. This would imply that the unified model for radio-loud quasars and radio galaxies could be valid at the highest radio luminosities.

5 SUMMARY

In this work, we have applied cross-correlation techniques to characterize the environments of $\sim$14 000 RLAGN with $P_{1.4\,GHz} > 10^{24}$ W Hz^{-1}, selected from $\sim$1.2 million LRG at $0.4 < z < 0.8$. We have also compared the clustering of RLAGN with that of radio-loud quasars over the same redshift interval. By using control samples of radio-quiet objects matched in redshift, stellar mass and optical luminosity (or radio luminosity, when appropriate) we have isolated the effect such parameters have on influencing the clustering signal. The main results of this paper can be summarized as follows:

(i) Radio AGN at $0.4 < z < 0.8$ are substantially more clustered than their parent luminous red galaxy population. RLAGN are also more strongly clustered than radio-quiet galaxies of the same stellar mass and redshift. The clustering differences are largest on scales less than 1 Mpc h^{-1}.

(ii) RLAGN hosted by more massive galaxies are more strongly clustered than those hosted by less massive galaxies. However, the clustering *difference* between RLAGN and control samples of radio-quiet galaxies is most pronounced for RLAGN in low-mass hosts.

(iii) We study the dependence of the clustering amplitude on the luminosity of the radio source. For $r_p > 1$ Mpc h^{-1} there is a weak, but significant anticorrelation with radio power. For $r_p < 1$ Mpc h^{-1} the dependence of clustering amplitude on luminosity is more complex: the cross-correlation amplitude increases with luminosity up to $\sim 10^{25.3}$ W Hz^{-1}, and then decreases for the most luminous radio sources in our sample.

(iv) We have compared the environments of RLAGN and RLQSOs. RLAGN are clustered more strongly than RLQSOs on all scales, indicating that they populate dark matter haloes of

Downloaded from http://mnras.oxfordjournals.org/ at Royal Observatory Library on November 20, 2014

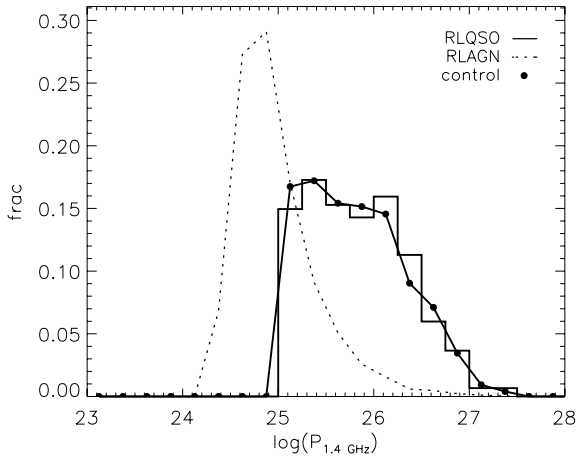

Figure 12. Normalized distributions of $\log(P_{1.4\,\mathrm{GHz}})$ for radio-loud AGN (dotted), radio-loud QSO (histogram) and control radio AGN (large dots) selected to have a similar distribution as of radio-loud quasars.

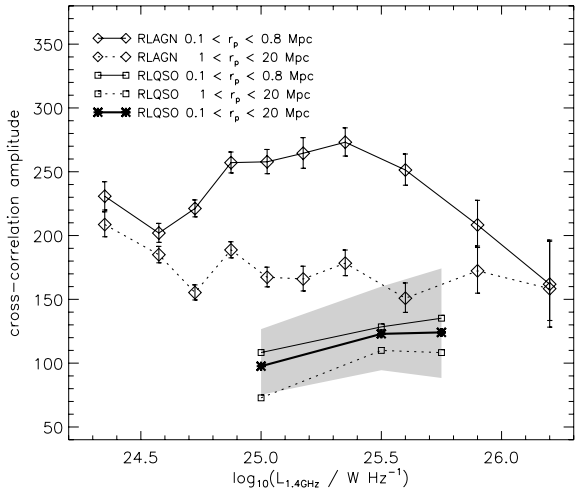

Figure 13. Change of the cross-correlation amplitude for RLAGN (diamonds) and RLQSO (squares), obtained by fitting a power law with varying amplitude and fixed exponent. Radio quasars are split in bins of increasing radio luminosity [$\log(P_{1.4\,\mathrm{GHz}}) > 25.0, > 25.5, > 25.75$]. Fits are calculated at two different spatial scales, $0.1 < r_\mathrm{p} < 0.8$ Mpc h^{-1} and $1 < r_\mathrm{p} < 20$ Mpc h^{-1}. A single fit over the range 1–20 Mpc h^{-1} is indicated by the thick line, enclosed by the shaded error region.

different mass. These results hold even when the RLAGN and RLQSO samples are matched in radio luminosity and black hole mass.

(v) There are indications that the most luminous RLAGN and RLQSOs in our sample ($P > 10^{26}$ W Hz^{-1}) do have similar clustering amplitudes. Only at these very high radio powers are the space-densities of radio-loud quasars and radio galaxies similar. This implies that unification of the two AGN populations may be valid above $P \sim 10^{26}$ W Hz^{-1}.

One major limitation of this study with regard to constraining AGN unification scenarios, is that it is based purely on photometric data from the SDSS, so we are unable to split our RLAGN sample into high-excitation and low-excitation sources. It is quite possible that the presence or absence of emission lines will provide the best way to define a population of radio galaxies that are clearly unified with the quasars. In this case, we would expect to find that the high-excitation radio galaxy population would cluster in a similar way to the quasars.

In addition, we note that because the parent sample of our RLAGN catalogue consists of luminous *red* galaxies, it is also likely that we miss some number of RLAGN with bluer colours and stronger emission lines. The analysis of the RLAGN luminosity function presented in Donoso et al. (2009) indicates that the missing sources cannot constitute more than ∼20 per cent of the total RLAGN population, so will not dominate the clustering signal of the radio AGN population as a whole. Nevertheless, the quasar analogues among the radio galaxy population may still be underrepresented in our analysis.

Fortunately, upcoming large spectroscopic surveys such as BOSS will target nearly complete samples of more than a million massive galaxies at $0.4 < z < 0.8$ and will provide optical spectra for tens of thousands of radio galaxies. We will then be able to quantify the fraction of RLAGN of given radio luminosity that have emission lines and to clarify how the clustering depends on emission line strength.

The most definitive result to emerge from our analysis is clear proof that the environment of a galaxy on the scale of the dark matter halo in which it resides (i.e. on scales of ∼1 Mpc h^{-1} and below) does play a key role in determining not only the probability that a galaxy is an RLAGN, but also the total luminosity of the radio jet. Mandelbaum et al. (2009) and Wake et al. (2008) also found that RLAGN were more strongly clustered than radio-quiet 'control' galaxies, but their RLAGN samples were too small to allow quantification of the trend with radio luminosity.

Combining our results with those of Best et al. (2005), we conclude that both black hole mass and environment must determine the radio-loud character of an active galaxy. This is in qualitative agreement with recent theoretical models that assume that RLAGN are fuelled by gas that cools at the centres of massive dark matter haloes (Croton et al. 2005, Bower et al. 2006, Merloni & Heinz 2008, Somerville et al. 2008, Fanidakis et al. 2009). In future work, we will examine in more detail whether the observational results are in quantitative agreement with the predictions of some of these models.

Our previous work also demonstrated that there is strong evolution in the space density of the radio AGN population only above a characteristic radio luminosity of $\sim 10^{25}$ W Hz^{-1} (Donoso et al. 2009). It is very intriguing that the results in this paper indicate that this luminosity marks the break point in clustering trends, and that the radio luminosity where denser environment ceases to favour the development of more luminous radio AGN, also is of order 10^{25} W Hz^{-1}.

Finally, the strong evolution of the radio source population at radio luminosities above $\sim 10^{25}$ W Hz^{-1} combined with the strong clustering of this population, must imply that the heating rate of the gas in groups and clusters of galaxies is higher at redshifts ∼0.5 than it is in the present day. We intend to quantify this in more detail in the upcoming work.

ACKNOWLEDGMENTS

We would like to thank the Max Planck Society for the financial support provided through its Max Planck Research School on Astrophysics PhD programme. PNB is grateful for support from the Leverhulme Trust.

Funding for the SDSS and SDSS-II has been provided by the Alfred P. Sloan Foundation, the Participating Institutions, the National Science Foundation, the US Department of Energy, the National

Downloaded from http://mnras.oxfordjournals.org/ at Royal Observatory Library on November 20, 2014

Aeronautics and Space Administration, the Japanese Monbukagakusho, the Max Planck Society and the Higher Education Funding Council for England. The SDSS website is http://www.sdss.org/. The SDSS is managed by the Astrophysical Research Consortium for the Participating Institutions. The Participating Institutions are the American Museum of Natural History, Astrophysical Institute Potsdam, University of Basel, Cambridge University, Case Western Reserve University, University of Chicago, Drexel University, Fermilab, the Institute for Advanced Study, the Japan Participation Group, Johns Hopkins University, the Joint Institute for Nuclear Astrophysics, the Kavli Institute for Particle Astrophysics and Cosmology, the Korean Scientist Group, the Chinese Academy of Sciences (LAMOST), Los Alamos National Laboratory, the Max-Planck-Institute for Astronomy (MPA), the Max-Planck-Institute for Astrophysics (MPIA), New Mexico State University, Ohio State University, University of Pittsburgh, University of Portsmouth, Princeton University, the United States Naval Observatory and the University of Washington.

This research project uses the NVSS and FIRST radio surveys, carried out using the National Radio Astronomy Observatory Very Large Array. NRAO is operated by Associated Universities, Inc., under cooperative agreement with the National Science Foundation.

REFERENCES

Antonucci R., 1993, ARA&A, 31, 473
Barr J. M., Bremer M. N., Baker J. C., Lehnert M. D., 2003, MNRAS, 346, 229
Barthel P. D., 1989, ApJ, 336, 606
Barthel P. D., Arnaud K. A., 1996, MNRAS, 283, 45
Becker R. H., White R. L., Helfand D. J., 1995, ApJ, 450, 559
Best P. N., 2004, MNRAS, 351, 70
Best P. N., Kauffmann G., Heckman T. M., Brinchmann J., Charlot S., Ivezić Ž., White S. D. M., 2005, MNRAS, 362, 25
Best P. N., von der Linden A., Kauffmann G., Heckman T. M., Kaiser C. R., 2007, MNRAS, 379, 894
Blanton M. R., Roweis S., 2007, AJ, 133, 734
Boroson T. A., 2002, ApJ, 565, 78
Böhringer H., Voges W., Fabian A. C., Edge A. C., Neumann D. M., 1993, MNRAS, 264, 25
Bower R. G., Benson A. J., Malbon R., Helly J. C., Frenk C. S., Baugh C. M., Cole S., Lacey C. G., 2006, MNRAS, 370, 645
Bruzual G., Charlot S., 2003, MNRAS, 344, 1000
Cannon R. D. et al., 2006, MNRAS, 372, 425
Coil A. L., Hennawi J. F., Newman J. A., Cooper M. C., Davis M., 2007, ApJ, 654, 115
Collister A. A., Lahav O., 2004, PASP, 116, 345
Collister A. et al., 2007, MNRAS, 365, 68
Condon J. J., Cotton W. D., Greisen E. W., Yin Q. F., Perley R. A., Taylor G. B., Broderick J. J., 1998, AJ, 115, 1693
Croom S. M. et al., 2005, MNRAS, 356, 415
Croton D. et al., 2005, MNRAS, 365, 11
Davis M., Peebles P. J. E., 1983, ApJ, 267, 465
da Ângela J. et al., 2008, MNRAS, 383, 565
Donoso E., Best P. N., Kauffmann G., 2009, MNRAS, 392, 617
Dunlop J. S., Peacock J. A., 1990, MNRAS, 247, 19
Fabian A. C., Sanders J. S., Allen S. W., Crowford C. S., Iwasawa K., Johnstone R. M., Schmidt R. W., Taylor G. B., 2003, MNRAS, 344, 43
Fanaroff B. L., Riley J. M., 1974, MNRAS, 167, 31
Fanidakis N., Baugh C. M., Benson A. J., Bower R. G., Cole S., Done C., Frenk C. S., 2009, preprint (arXiv:0911.1128)
Franceschini A., Vercellone S., Fabian A. C., 1998, MNRAS, 297, 817
Hamilton A. J. S., 1993, ApJ, 417, 19
Hardcastle M. J., 2004, A&A, 414, 927
Hardcastle M. J., Evans D. A., Croston J. H., 2006, MNRAS, 370, 1893
Hardcastle M. J., Evans D. A., Croston J. H., 2007, MNRAS, 376, 1849
Häring N., Rix H. W., 2004, ApJ, 604, 89
Heckman T. M., Kauffmann G., Brinchmann J., Charlot S., Tremonti C., White S. D. M., 2004, ApJ, 613, 109
Hickox R. C. et al., 2009, ApJ, 696, 891
Hill G. J., Lilly S. J., 1991, AJ, 367, 1
Hine R. G., Longair M. S., 1979, MNRAS, 188, 111
Ho L. C., 2002, ApJ, 564, 120
Jackson C. A., 1999, Publ. Astron. Soc. Australia, 16, 124
Kauffmann G. et al., 2003, MNRAS, 341, 33
Kauffmann, Guinevere,Heckman T. M., Best P. N., 2008, MNRAS, 384, 953
Kellermann K. I., Sramek R., Schmidt M., Shaffer D. B., Green R., 1989, AJ, 98, 1195
Lacy M., Laurent-Muehleisen S. A., Ridgway S. E., Becker R. H., White R. L., 2001, ApJ, 551, 17
Laing R. A., Wall J. V., Jenkins C. R., Unger S. W., 1994, ed., ASP Conf. Ser. Vol. 54, The Physics of Active Galaxies. Astron. Soc. Pac., San Francisco, p. 201
Lawrence A., 1991, MNRAS, 252, 586
Ledlow M. J., Owen F. N., 1996, AJ, 112, 9
Li C., Kauffmann G., Jing Y. P., White S. D. M., Börner G., Cheng F. Z., MNRAS, 2006a, 368, 21
Li C., Kauffmann G., Wang L., White S. D. M., Heckman T. M., Jing Y. P., 2006b, MNRAS, 373, 457
Li C., Kauffmann G., Heckman T. M., Jing Y. P., White S. D. M., 2008, MNRAS, 385, 1903
Mandelbaum R., Li C., Kauffmann G., White S. D. M., 2009, MNRAS, 393, 377
McNamara B. R. et al., 2000, ApJ, 534, L135
Merloni A., Heinz S., 2008, MNRAS, 388, 1011
Metacalf R. B., Magliocchetti M., 2006, MNRAS, 365, 101
Miley G. K. et al., 2006, ApJ, 650, 29
Padmanabhan N., White M., Norberg P., Porciani C., 2009, MNRAS, 397, 1862
Peebles P. J. E., 1980, The Large-scale Structure of the Universe. Research supported by the National Science Foundation. Princeton Universtity Press, Princeton, NJ
Pentericci L. et al., 2000, A&A, 361, 25
Porciani C., Norberg P., 2006, MNRAS, 371, 1824
Prestage R. M., Peacock J. A., 1988, MNRAS, 230, 131
Richards G. T. et al., 2002, AJ, 123, 2945
Schneider D. P. et al., 2007, AJ, 134, 102
Shen Y., Greene J. E., Strauss M. A., Richards G. T., Schneider D. P., 2008, ApJ, 680, 169
Shen Y. et al., 2009, ApJ, 697, 1656
Sheth R. K., Tormen G., 1999, MNRAS, 308, 119
Simpson C., 1998, MNRAS, 297, 39
Smith E. P., Heckman T. M., 1990, AJ, 348, 38
Snellen I. A. G., Lehnert M. D., Bremer M. N., Schilizzi R. T., 2003, MNRAS, 342, 889
Somerville R. S., Hopkins P. F., Cox T. J., Robertson B. E., Hernquist L., 2008, MNRAS, 391, 481
Stocke J. T., Morris S. L., Weymann R. J., Foltz C. B., 1992, ApJ, 396, 487
Stoughton C. et al., 2002, AJ, 123, 485
Urry M. C., Padovani P., 1995, PASP, 107, 803
Yates M. G., Miller L., Peacock J. A., 1989, MNRAS, 240, 129
York D. G. et al., 2000, AJ, 120, 1579
Wake D. A., Croom S. M., Sadler E. M., Johnston H. M., 2008, MNRAS, 391, 1674
Wold M., Lacy M., Lilje P. B., Serjeant S., 2000, MNRAS, 316, 267

This paper has been typeset from a TEX/LATEX file prepared by the author.

Downloaded from http://mnras.oxfordjournals.org/ at Royal Observatory Library on November 20, 2014